CAM_{ID}: An Assuasive Approach to Reveal Source Camera through Inconspicuous Evidence

Abstract

Identifying the source camera of digital images is an important problem due to the abundance of such images nowadays. Although photo response non-uniformities (PRNUs) can accurately identify the source camera, seam-carving techniques have been introduced to hide the cameras' identity by invalidating the positional correspondence assumption in the PRNU. Especially, the seam carving techniques create irregular carving patterns, which makes source camera identification from seam-carved images challenging. In this paper, we propose a feature-based method called CAM_{1D}, to identify the source camera of seam-carved images. CAM_{1D} constructs a series of camera signatures to enhance robustness and reliability, rather than relying on a single PRNU for identification. Useful features are extracted from the correlation between a series of camera signatures and seam-carved photos, giving high source camera identification accuracy. Experimental results using the confusion matrix and F1 score confirm the effectiveness of CAM_{1D}.

Keywords: source-camera identification; photo response non-uniformity noise; seam-carving; digital image forensics

1. INTRODUCTION

Nowadays, the authentication of digital images is a crucial issue that involves two branches: source camera identification and forgery detection. The former aims to determine the camera that has been used to capture a photo (Bernacki 2020), while the latter focuses on detecting any manipulations and alterations made to the image content (Birajdar and Mankar 2013).

Extensive research has been conducted on photo response non-uniformity (PRNU) for source camera identification. Based on the fact that the PRNU can uniquely identify a camera, PRNU can be used as a camera signature (Chen et al 2008; Lukáš, Fridrich, and Goljan 2006). Numerous studies have been conducted to enhance the extraction and robustness of PRNU (Chan et al. 2013; Shi et al 2017; Lau et al 2015; Kang et al 2012). It has been found that commonly used image processing techniques, such as enhancement and compression, do not alter the uniqueness of the PRNU in identifying the source device. However, cropping and resizing can significantly impact the PRNU, as these modifications cause the pattern noise in the modified image to be misaligned with the PRNU. Despite this, if the entire image is subjected to cropping and resizing, and the transformation parameters are known, PRNU is still able to identify the source device (Akbari et al 2022; Law and Law 2022).

Seam carving is an alternative method for image resizing and scaling that removes visually unimportant elements and keeps visually important regions in an image. Seams represent visually unimportant pixels that can be eliminated to reduce the image size. These seams typically run through smooth regions of the image, as illustrated in Fig 1. Fig 1(a) shows the original image while Fig 1(b) shows the locations of

seams (represented using red color). We can see that these seams avoid running through visually important regions in the original image. By removing these seams, the resized image is formed as shown in Fig 1(c).

(a) (b) (c)

Fig 1: (a) the original image, (b) the positions of seams (in red color), and (c) the resized image after removing the seams.

Since the smooth or unimportant elements in an image are not located in the same position across different photos, seams' positions change from one image to another as shown in Fig 2. Thus the resizing pattern is irregular and is image content dependent. It is difficult to know which pixels have been removed from the original image to form the resized image. In this case, it is not an easy task to perform the PRNU-based source camera identification on seam-carved photos.

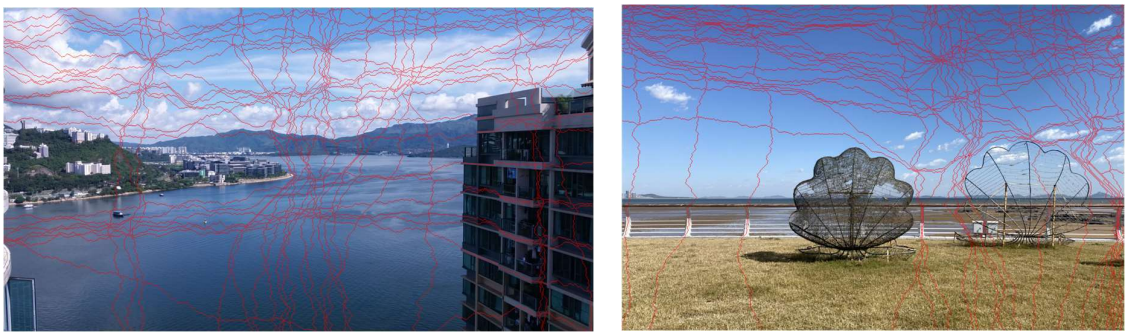

(a) (b)

Fig 2: Seam positions (in red colors) vary with different images.

To further illustrate the effect of seam carving on source camera identification, let us consider an example of a small 8x8 image. Fig 3(a) shows the layout of the 8x8 image, with *R*ij representing individual pixel values. Suppose that two vertical seams are identified and removed to create an 8x6 image. Depending on the image content, the seam positions can be different in these two images, as shown in Figs 3(b) and 3(c). As a result, the noise patterns of the two resulting images do not fully align with each other in the 8x6 image. Without knowing the exact seam locations, it is not possible to identify the corresponding noise residues. This makes PRNU-based source identification a challenging task for seam-carved images.

R11	R12	R13	R14	R15	R16	R17	R18
R21	R22	R23	R24	R25	R26	R27	R28
R31	R32	R33	R34	R35	R36	R37	R38
R41	R42	R43	R44	R45	R46	R47	R48
R51	R52	R53	R54	R55	R56	R57	R58
R61	R62	R63	R64	R65	R66	R67	R68

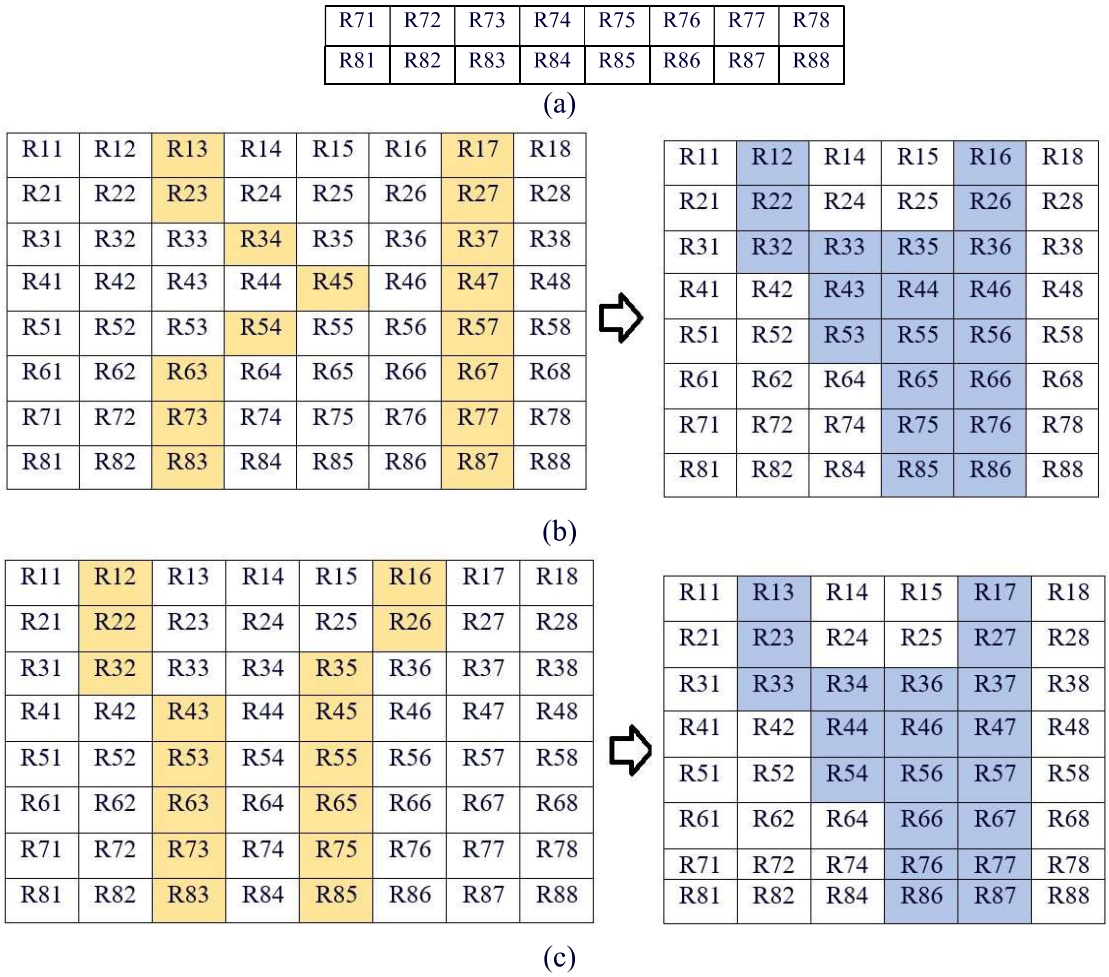

Fig 3: (a) A small 8x8 image, (b) and (c) show the locations of the vertical seams in two images with different image contents which are highlighted using yellow color, and the resultant 8x6 resized images after removing the two vertical seams. The blue color is used to highlight those pixels with non-aligned noise residues.

The first study on source camera identification of seam-carved images was in 2013 (Bayram, Sencar, and Memon 2013). Its idea is to use uncarved blocks in the resized image for source identification as the noise residues in these uncarved blocks are fully aligned with the original PRNU. It is found that reliable identification can be achieved if the uncarved blocks are larger than 50×50 pixels. In another study, blocks from multiple seam-carved images captured from the same camera device can be integrated to provide reliable identification (Taspinar, Mohanty, and Memon 2016; Taspinar, Mohanty, and Memon 2017).

These studies (Bayram, Sencar, and Memon 2013; Taspinar, Mohanty, and Memon 2016; Taspinar, Mohanty, and Memon 2017) provide a feasibility study on source identification of seam-carved photos. More research is needed to understand how uncarved blocks can be identified and integrated in practice, and how source identification can be performed more effectively. This research study aims to investigate the following research questions:

- How can we identify potential uncarved blocks in a seam-carved image?

- Can we extract reliable features that enable us to link a seam-carved image to its source camera?

We studied the correlation between the photo and the camera signature and found that different patterns were obtained depending on whether the seam-carved photos were captured by their source cameras. We then investigated how reliable features can be extracted from the correlation pattern to link a seam-carved image to its source camera. This study makes the following contributions.

- We observed that the correlation pattern between the noise residues and PRNU differed significantly between matched and unmatched cases. The correlation patterns can be used for reliable source identification.
- A feature-based source identification method for seam-carved images (CAM_{ID}) was developed. The reliability of the method was demonstrated experimentally.

The remainder of this paper is organized as follows. Section 2 reviewed the PRNU-based source camera identification and seam-carving. An analysis of the correlation patterns is given in Section 3. Our proposed method CAM_{ID} is then described in Section 4. The simulation results are presented in Section 5. Finally, Section 6 concludes the paper.

2. BACKGROUND

2.1 Source Camera Identification

Source camera identification attempts to link a photo to the device that captured it. The most popular feature for source camera identification is the photo response non-uniformity (PRNU) noise. As this noise originates from sensor defects due to manufacturing imperfections, PRNU is unique for each camera device. In other words, the PRNUs of two camera devices are different, even if the two devices are from the same brand and model (Chen et al. 2008; Lukáš; Fridrich, and Goljan 2006).

The PRNU of camera device A is obtained using N images taken by A through approaches such as averaging noise residues (Lukáš, Fridrich, and Goljan 2006) or maximum likelihood estimation (Chen et al. 2008). After PRNU is estimated, it can be used as a camera signature. The noise residue in any photo taken by a camera should be similar to that of the camera PRNU. Mathematically, the peak-to-correlation value (PCE) can be used to quantify the similarity between camera A's PRNU (denoted as $K_A(N)$) and the test photo I_t (Goljan et al 2009). It is defined as,

$$PCE(K_A(N), I_t) = \frac{C(0,0)^2}{\frac{1}{S_x S_Y - |\Omega|} \sum_{(u,v) \notin \Omega} C(u,v)^2} \quad (1)$$

where S_x and S_Y are the width and the height of the image, Ω denotes a small neighbor around (0,0), C is the correlation matrix between $K_A(N)$ and the noise residue in I_t. It is expressed as,

$$C = \left(K_A(N) - \overline{K_A(N)}\right) \cdot (w_t - \overline{w_t}) \quad (2)$$

where a bar over a symbol represents its mean value, $\cdot$ denotes the dot product and the noise w_t is the difference between the test photo and its denoised version, i.e.,

$$w_t = I_t - D(I_t) \tag{3}$$

where $D(.)$ is the denoising operator (Chan et al. 2013; Shi et al 2017; Lau et al 2015; Liu et al 2014). Let $\{I_i^A, i = 1, \ldots, N\}$ be the sequence of N images captured by A. The PRNU $K_A(N)$ is constructed through denoising and averaging as,

$$K_A(N) = \frac{1}{N}\sum_{i=1}^{N}(I_i^A - D(I_i^A)) \tag{4}$$

In source camera identification, N must be at least 30 to provide a reliable camera signature (Chen et al. 2008). While PRNU can reliably identify the source of an image even after common image processing operations and compression, its main limitation lies in its requirement for positional dependence; w_t must be completely aligned with $K_A(N)$. Even a one-pixel misalignment causes PRNU-based source identification method to fail (Irshad et al 2023; Liu et al 2021).

2.2 Study of Seam-carving Methods

Seam-carving is a content-aware image-resizing method in which visually important regions are preserved while those unimportant areas are removed to achieve image resizing (Avidan and Shamir 2007). Gradient magnitude is used to define how important a region is. Highly textured regions with large variations in pixel intensity (i.e., large gradient magnitudes) are not resized, whereas smooth regions with small gradient magnitudes are removed. In this way, visual artifacts arising from resizing operations can be minimized. Mathematically, the absolute gradient magnitude $e(I)$ of an image I is defined as,

$$e(I) = \left|\frac{\partial}{\partial x} I\right| + \left|\frac{\partial}{\partial y} I\right| \tag{5}$$

where $\frac{\partial I}{\partial x}$ and $\frac{\partial I}{\partial y}$ denote the partial derivatives of the image in the horizontal and vertical directions respectively, and $|.|$ indicates an absolute value. A large $e(I)$ value corresponds to regions with large changes in intensity values that should not be scaled. A small $e(I)$ value implies smooth regions that can be removed without any obvious visual distortions.

Seam-carving involves computing a path connecting low-energy pixels in an image. The path of pixels having the minimum total energy is named "seam" (Frankovich and Wong 2011). Images can be enlarged by copying and repeating seams or shrunk by removing seams without disturbing important image structures. Fig 1 shows an example. As can be seen in Fig 1(b) and Fig 2, seams are located in smooth regions and do not run across high-energy regions. With repeated removal of these seams, image size can be reduced as shown in Fig 1(c).

2.3 Source Camera Identification in Seam-carved Photos

When seams are removed, the remaining pixels were shifted to fill the gaps. This process is shown in Fig 3. Figs 3(b) and 3(c) represent two different photos taken by the same camera. Due to their different scene content, seam positions can be different. As a result, the resized image would have different pixels removed. As evidenced in Figs 3(b) and 3(c), the pixel-to-pixel positional correspondence between the noise residues and the camera PRNU was destroyed. The seams removal process gives an irregular pattern that is dependent on the scene content. As a result, it is challenging to do any transformation to re-establish the positional correspondence. The misalignment would cause the PCE value between the camera PRNU and the noise residue of the seam-carved photo to be very small.

The first study on source camera identification of seam-carved photos was in 2013 (Bayram, Sencar, and Memon 2013). It is based on the idea that high-energy regions are less likely to be affected by seam carving and thus these regions may contain some parts of the original PRNU. If these "uncarved" blocks are larger than 50x50 pixels, reliable source identification can be achieved in some cases (Bayram, Sencar, and Memon 2013). If the uncarved blocks are smaller than 50x50 pixels, multiple uncarved blocks have to be combined to give a better estimation. The number of blocks required varied greatly with individual camera devices. In some devices, using more than 500 blocks is still not enough to give accurate identification (Dirik, Sencar, and Memon 2014). Practically, a study on how the uncarved blocks in the image are found should be conducted.

Instead of considering only one seam-carved image, multiple seam-carved images captured from the same camera can be considered (Taspinar, Mohanty, and Memon 2017). The identification performance depends on the randomness of seam positions, the number of seams removed, and the total number of seam-carved images available. For example, when a seam is carved from a 25x25 image block and the seam movement is restricted to be within a 25x25 block, accurate identification can be achieved with 5 seam-carved images. However, when the movement is unrestricted with 128 horizontal and vertical seams removed, more than 100 seam-carved images are required (Taspinar, Mohanty, and Memon 2017). This shows that it is challenging to use the PRNU-based method for source camera identification on seam-carved images. A reliable method is required to perform source camera identification on seam-carved photos.

3. PCE Pattern Analysis

In source camera identification, $PCE(K_A(N), I_t)$ in eq (1) is used to characterize the similarity between the test photo and the camera signature. If the PCE value is larger than a threshold (e.g., 50), it is likely that the test photo I_t was taken by camera device A. We consider two cases:

Matched case: the test photo is from the source camera.
Unmatched case: the test photo is not from the source camera.

We found that the changes in $PCE(K_A(N), I_t)$ with respect to N (the number of images used to construct the camera signature PRNU) are very different in the matched (Fig 4(a)) and the unmatched cases (Fig 4(b)). Five cameras in Table 1 were considered. Note that two cameras are different devices from the same camera model. Fig 4(a) shows $PCE(K_A(N), I_t)$ when I_t is from camera A (i.e., the matched case) while Fig 4(b) is for I_t from cameras other than A (i.e., the unmatched case).

In the matched case in Fig 4(a), the PCE value is always large. When N is 30, the PCE value is greater than 50 for most camera devices. Thus, one can be confident that the test photo came from a particular camera device. This explains why, in the traditional approach, N can be fixed at 30 to produce a single PCE value for reliable identification (Taspinar, Mohanty, and Memon 2016).

In the unmatched case in Fig 4(b), the PCE values do not show an increasing trend with N. The PCE values are always smaller than 10 no matter how large N is. We can thus see that the trend of PCE is very different in the matched and the unmatched cases. Increasing the number of photos N to construct the camera signature $K_A(N)$ will increase the PCE values in the matched case, but not the unmatched case.

Next, we investigate how this trend changes for seam-carved photos. As discussed, seam-carving destroys the pixel-to-pixel correspondence between the PRNU and noise residue. Figs 4(c) and 4(d) show the changes in the PCE values for the matched cases in the seam-carved photos; while Fig 4(e) shows the trend for the unmatched case.

As shown in Fig 4(c) for the matched case, the PCE value decreases if the image has been seam-carved. Even when N is 120, the PCE value is less than 50 for some of the cameras. Thus, seam carving makes it difficult to perform reliable source camera identification using a single PCE value irrespective of how large N is. Despite that, Fig 4(c) illustrates that PCE values increase with N, even for seam-carved images. Although using a single PCE value for source identification in seam-carved photos is unreliable, the trend in the PCE values can be considered.

Taspinar, Mohanty, and Memon 2017 proposed a very challenging anonymization scheme called the forced seam carving in which at least one seam is removed inside every 25 × 25 image block. Fig 4(d) shows the PCE values in the matched case when this forced seam carving method is used. We can see that the PCE value decreases significantly for the forced seam carving method (as compared to Fig 4(c)). It would be very challenging to perform source camera identification using a single PCE value. Despite that, the trend of the PCE values is still increasing.

Fig 4(e) shows the unmatched case in the seam-carved photos. We considered both the traditional seam-carved method and the forced seam-carved method in this diagram. Unlike the matched case in Figs 4(c) and 4(d), the PCE values do not show an increasing trend with N for the seam-carved photos not captured by the same device as $K_A(N)$.

In summary, a camera can be identified using a single PCE value if the image does not undergo seam-carving. For seam-carved photos, using a single PCE value is unreliable. It is better to consider the trend of the PCE values instead. In the following, a feature-based source camera identification method using PCE trend information is proposed for seam-carved photos.

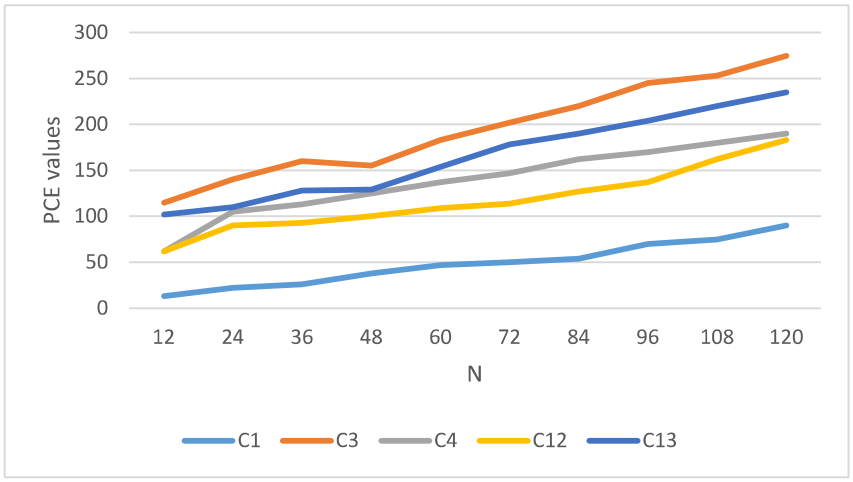
300
250
200
150
100
50
0
PCE values
12
24
36
48
60
72
84
96
108
120
N
C1
C3
C4
C12
C13

(a)

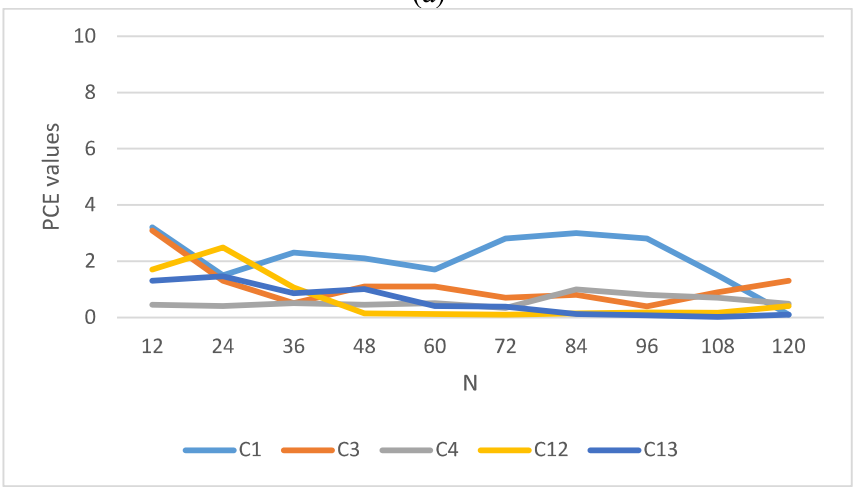
10
8
6
4
2
0
PCE values
12
24
36
48
60
72
84
96
108
120
N
C1
C3
C4
C12
C13

(b)

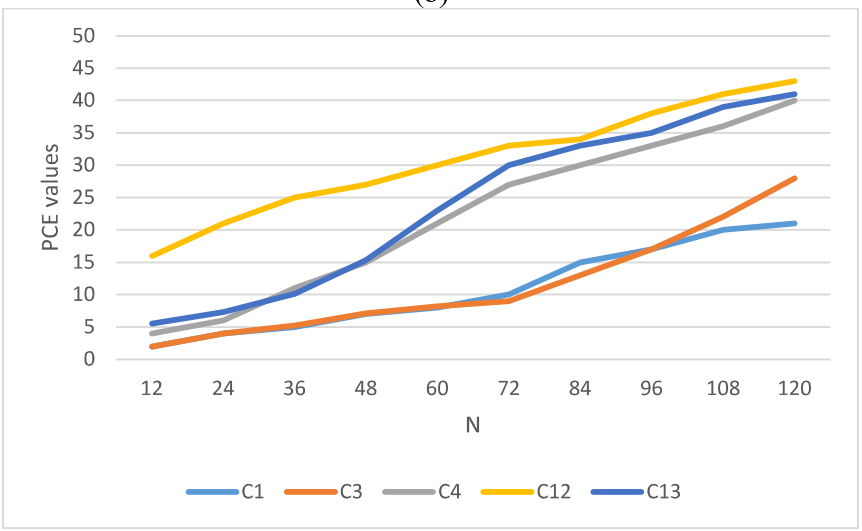
50
45
40
35
30
25
20
15
10
5
0
PCE values
12
24
36
48
60
72
84
96
108
120
N
C1
C3
C4
C12
C13

(c)

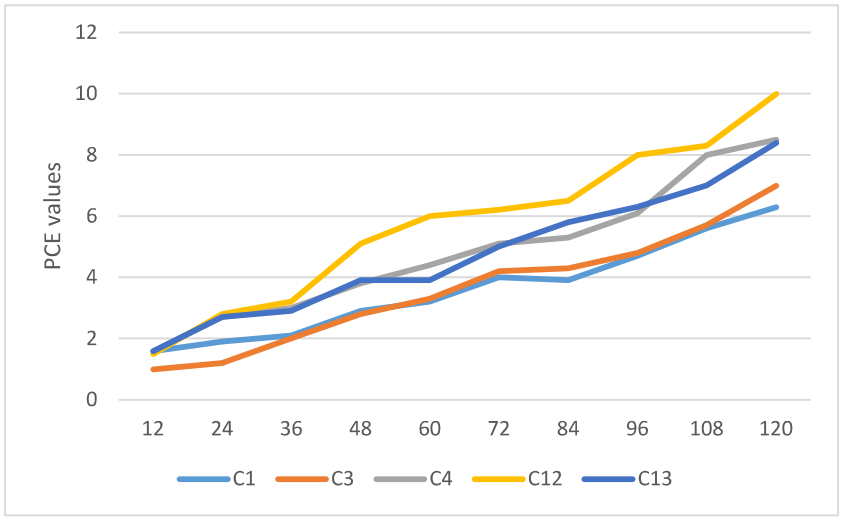

(d)

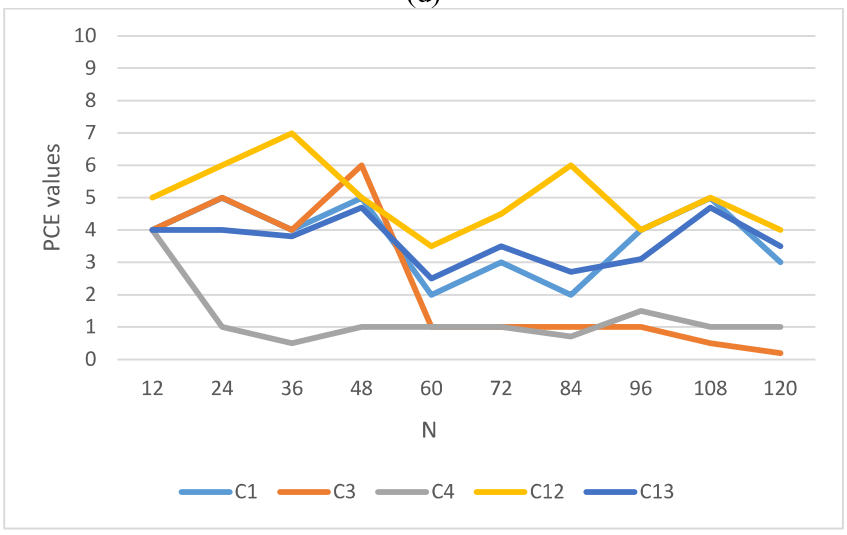

(e)

Fig 4: Plot of $PCE(K_A(N), I_t)$ against N for (a) matched cases of unmodified images; (b) unmatched cases of unmodified images; (c) matched cases of seam-carved photos, (d) matched cases of forced seam-carved photos, and (e) unmatched cases.

4. The Proposed Method, CAM$_{1D}$

4.1 Methodology

Seams are often located in low-energy regions. As such, uncarved blocks, i.e., blocks without seam removals, can only be found in high-energy regions. Uncarved blocks are important in source camera identification because positional correspondence with camera signature PRNU can be maintained within these blocks. However, high-energy regions are those highly textured regions that are unreliable for source camera identification. As discussed in Section 3, several PRNUs constructed from different numbers of images are needed to improve the reliability of source camera identification. Fig 5 summarizes the key steps of the proposed method CAM$_{1D}$.

The proposed method CAM_{ID} contains two parts: camera signature construction and source camera identification in seam-carved photos. We consider a closed-set problem in which the test photo was taken by one of the cameras under testing. Assume that there are L cameras under testing, $\{C_i, i = 1, \cdots, L\}$ and each camera has M images. These M images are randomly divided into r groups, with m number of images in a group, i.e., $M=r*m$. For each camera C_i, a set of signatures constructed from different numbers of images can be obtained in the offline camera signature construction step as $\{K_{C_i}(m), K_{C_i}(2m), \ldots, K_{C_i}(rm)\}$ according to Eq. (4).

The second part of source camera identification in seam-carved images comprises three components: (1) block selection in the seam-carved image, (2) feature extraction, and (3) final prediction. A suitable block is selected for source camera identification. Features are then extracted from the block, and a decision score is obtained to determine whether the seam-carved test photo comes from a specific camera. These steps are described in the following subsections.

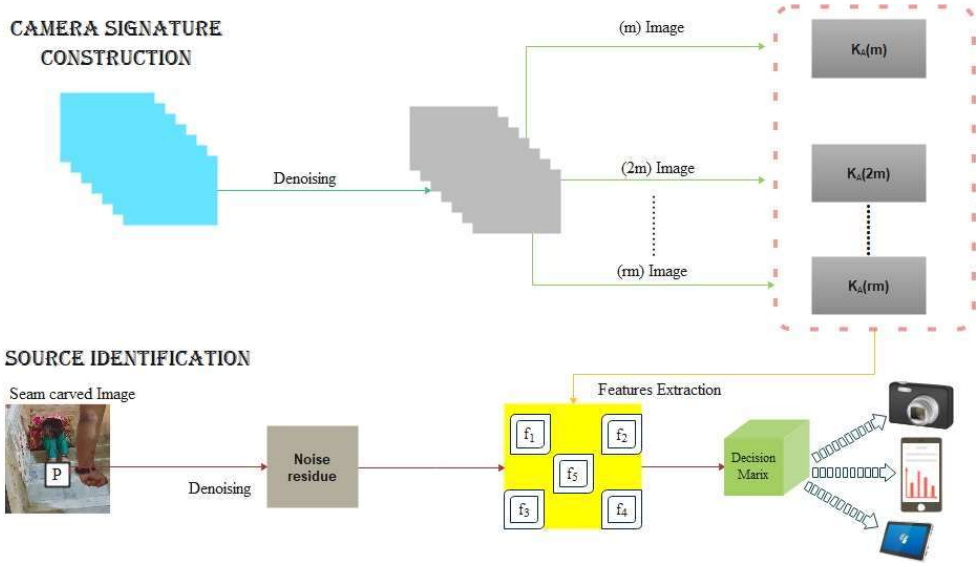

Fig 5: Flowchart of the proposed method CAM_{ID}

4.2 Block Selection

Uncarved blocks are important in source camera identification because positional correspondence with the camera signature PRNU can be maintained within these blocks. In block selection, a block with a high probability of containing uncarved sub-blocks is identified. As seems seldom run across a highly textured area or regions with edges, these regions are less likely to be seam-carved. The gradient magnitude can be used to identify these blocks. The seam-carved test image is first divided into several blocks. The sum of the vertical and horizontal gradient magnitude inside each block is obtained. Let P be the block with the greatest energy of all blocks. Due to its large energy, P likely contains uncarved sub-blocks that can be used for source camera identification. Fig 6 shows an example of such a block that contains a highly textured area.

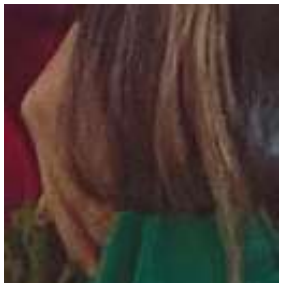

Fig 6: Example of block *P* with a size of 128 × 128.

4.3 Feature Extraction

The size of *P* is much smaller than that of the camera signature PRNU. A search is performed within the search window in the *r* camera signatures $\{K_{C_i}(m), K_{C_i}(2m), \dots, K_{C_i}(rm)\}$ to find the potential correspondence position between *P* and each of the PRNUs, $K_{C_i}(jm)$. Mathematically, the PCE value between the *r* camera signature and the block *P*, $PCE(K_{C_i}(N), P)$, is obtained. Of all locations within the search window, the maximum PCE value was obtained. We define the maximum PCE within the search window as $Q(jm, C_i)$, and its corresponding matched position as $p(jm, C_i)$. In this way, we obtained a set of PCE values $Q = \{Q(m, C_i), Q(2m, C_i), \dots, Q(rm, C_i)\}$ and matched positions $\{p(m, C_i), p(2m, C_i), \dots, p(rm, C_i)\}$ for $\{C_i, i = 1, \dots, L\}$.

As discussed in Section 3, the trend in the set of PCE values $\{Q(m, C_i), Q(2m, C_i), \dots, Q(rm, C_i)\}$ should be upward if the test photo is captured by the camera C_i (Figs 4(c) and 4(d)). Otherwise, the trend is random (Fig 4(e)). Five features were extracted to quantify this phenomenon. They are defined as follows:

(1) The sum of the PCE values,

$$f_1 = \sum_{j=1}^{r} Q(jm, C_i) \tag{6}$$

f_1 indicates the total correlation with all camera signatures $\{K_{C_i}(m), K_{C_i}(2m), \dots, K_{C_i}(rm)\}$. It should be large if the seam-carved test photo is from the camera C_i.

(2) The overall change in the PCE value, i.e., the trend of the PCE value when *N* (the number of photos to construct the camera signature) increases.

$$f_2 = Q(rm, C_i) - Q(m, C_i) \tag{7}$$

f_2 captures the trend in the PCE values. With the upward trend shown in Figs 4(c) and 4(d), f_2 is large if the seam-carved test photo is obtained from the camera C_i. With the random trend in Fig 4(e), f_2 is small if the seam-carved test photo is obtained from cameras other than C_i.

(3) The absolute difference of the change in the matched location,

$$f_3 = \sum_{j=1}^{r-1} |p((j+1)m, C_i) - p(jm, C_i)| \tag{8}$$

f_3 denotes the change in matched location. If the seam-carved test photo is from the camera C_i, the matched location should be relatively stable no matter how many images are used to construct the camera signature. Thus, f_3 must be small.

(4) We define β_j as the sharpness of the maximum correlation value $Q(jm, C_i)$ compared to its 20×20 neighbors. Owing to the positional correspondence relationship, the peak correlation value should be much larger than that of its neighbors if the seam-carved test photo is from the camera C_i. β_j is defined as,

$$\beta_j = \sum_{x=0}^{19} \sum_{y=0}^{19} \frac{(Q(jm, C_i) - |M(x,y)|)^2}{Q(jm, C_i)^2} \tag{9}$$

where $M(x,y)$ is the 20 × 20 sub-block of $PCE(K_{C_i}(jm), P)$, centered at the matched location $p(jm, C_i)$. The fourth and fifth features capture characteristics related to the sharpness of the maximum correlation value. They are defined as,

$$f_4 = \sum_{j=1}^{r} \beta_j \tag{10}$$

and

$$f_5 = \beta_r - \beta_1 \tag{11}$$

If the seam-carved test photo is from the camera C_i, the peak $Q(jm, C_i)$ should be sharp, and f_4 should be large. When more images were used to construct the camera signature, the peak became more prominent. As a result, β_j should increase with j, and f_5 should be large.

These five features capture the characteristics of the changes associated with the camera signatures $\{K_{C_i}(m), K_{C_i}(2m), \ldots, K_{C_i}(rm)\}$. Instead of examining a single PCE value, these features can reliably characterize the source camera information left in the seam-carved photo.

4.4 Decision Metric

The decision metric was used to determine which camera device in $\{C_i, i = 1, \dots, L\}$ was used to capture the seam-carved test photo. For each camera C_i, we have a set of features $\{f_n(C_i), n = 1, \dots, 5\}$. Min-max normalization was adopted so that the normalized features are between 0 and 1.

$$\tilde{f}_n(C_i) = \frac{f_n(C_i) - \min\limits_{C_i} f_n(C_i)}{\max\limits_{C_i} f_n(C_i) - \min\limits_{C_i} f_n(C_i)} \tag{12}$$

for *n*=1 to 5. These five normalized features characterize the change in PCE values from different perspectives. They are combined to give a final decision score as follows,

$$Y = W_1\tilde{f}_1 + W_2 x_2 \tilde{f}_2 - W_3\tilde{f}_3 + W_4\tilde{f}_4 + W_5\tilde{f}_5 \tag{13}$$

The entropy weighting method was used to determine the weighting coefficient W_n (Minnen et al. 2018). In this method, entropy is used to set the weights, as it can indicate the distribution of the feature values.

$$W_n = \frac{1 - e_n}{\sum_{l=1}^{5} 1 - e_l} \tag{14}$$

where e_n is the scaled entropy obtained from $\tilde{f}_n$.

$$e_n = -\sum_{i \in \{1,\cdots,L\}} P_{n,c_i} \, log_5(P_{n,c_i}) \tag{15}$$

and

$$P_{n,c_l} = \frac{\tilde{f}_n(C_i)}{\sum_{i \in \{1,\cdots,L\}} \tilde{f}_n(C_i)} \tag{16}$$

A large *Y* indicates that the test photo was likely taken by the particular camera.

4.5 An illustrative example

In this part, the effectiveness of the proposed five features on source camera identification of seam-carved photos is discussed. As shown in Figs 4(c) and 4(d), even when *N*=120, the PCE values between the camera signature and the seam-carved photos are always smaller than 50. Thus, for all these cameras, reliable source camera identification cannot be done using a single camera signature. The five features proposed in Section 4.3 attempt to provide an alternative approach for source camera identification.

Boxplots are used to illustrate the variation of these five features in the matched and unmatched cases. Matched case means that the test photos come from the same camera as the camera signature. Fig 7 shows these boxplots. Figs 7(a) and 7(b) show respectively the f_1 and the f_2 values. We can see that in general f_1 and f_2 values in the matched case are much larger than those in the unmatched case. This is expected because the total PCE values (i.e., f_1) in the matched case should be larger than those in the unmatched case. Similarly, the trend in the PCE value in the matched case should be upward resulting in a large f_2 value.

Fig 7(c) shows the boxplot of f_3. The f_3 value indicates the change in the matched location. In the matched case, the values are always zero while there are much larger variations in the unmatched case.

The features f_4 and f_5 attempt to characterize the sharpness of the PCE values in a local region. As shown in Figs 7(d) and 7(e), the distribution of these values in the matched and unmatched cases is not the same. Fig 7 empirically demonstrates the effectiveness of these five features. While individual features may not be sufficient for reliable source camera identification on seam-carved photos, these five features can be integrated to devise a decision metric as in eq (13) and Fig 8.

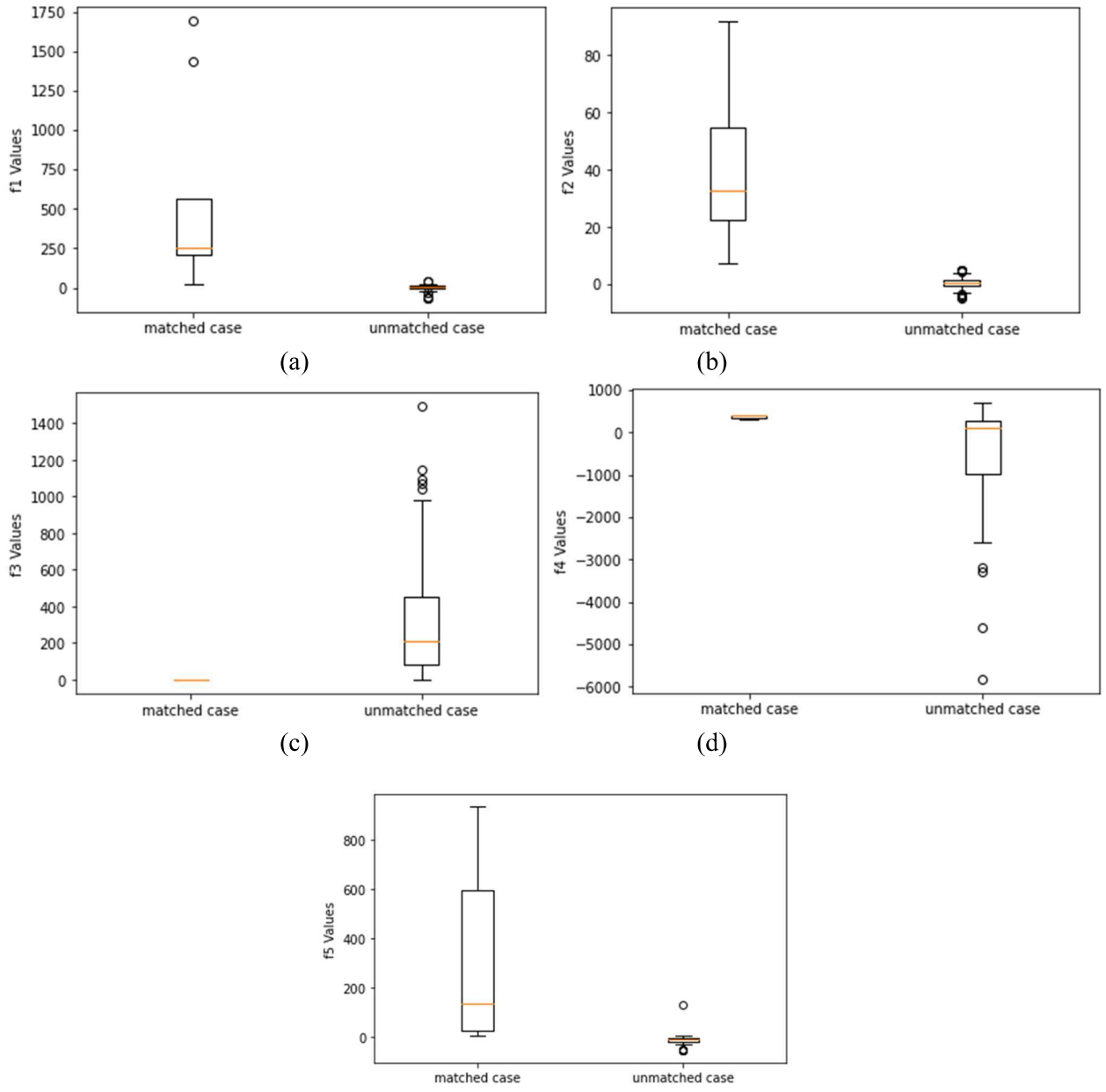

Fig 7: Boxplots of the five features, (a) f_1, (b) f_2, (c) f_3, (d) f_4 and (e) f_5 in the matched and unmatched case. The matched case means that the test photo comes from the same camera as the camera signature while the unmatched case means that the test photo does not come from the same camera as the camera signature.

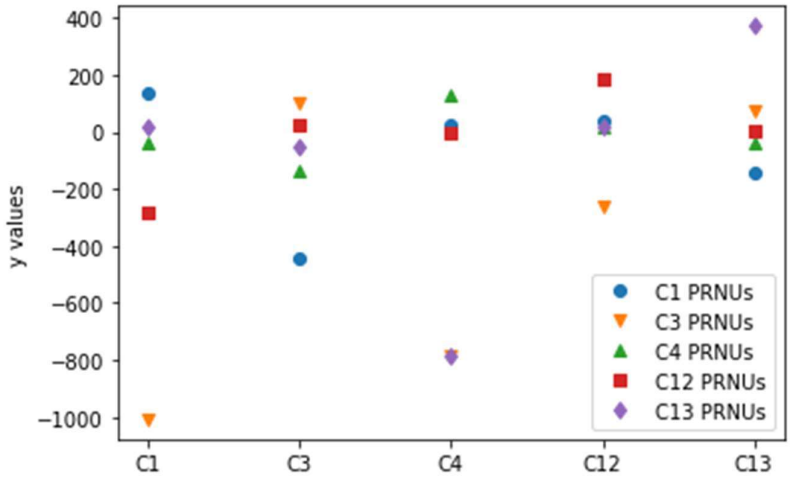

Fig 8: The *Y* values obtained. The horizontal axis shows the specific camera used to take the test photo.

Fig 8 shows the decision score (Y values). The horizontal axis shows the camera that has been used to obtain the test photos. In the first column "C1", we can see that the highest value is around 140 which corresponds to the camera signature C_1. Thus, the *Y* value obtained for test photo C_1 achieves the highest with the camera signature of C_1. A similar observation is obtained for the other cameras in the next four columns of Fig 8. Note that we considered a closed-set scenario in our experimental setting. If the matching camera is not known, i.e., an open-set scenario, we may need to set a threshold for the minimum decision score for the matching case.

5. Experimental results

5.1 Dataset construction

To the best of our knowledge, there is no public image database specifically designed for source camera identification of seam-carved images. Despite that, VISION and Dresden are two popular databases in source camera identification (Gloe and Böhme 2010, Shullani et al. 2017). We thus used images from these datasets for preliminary analysis. Both datasets have a variety of content, containing natural scenes and man-made objects in indoor and outdoor environments. Table 1 shows the cameras used in our experiments. The camera brand and model, the number of images, and their resolutions are shown. Note that Samsung_NV15_0 and Samsung_NV15_1 are two different devices from the same camera brand and model. There are 120 images from each camera device. These images are further randomly divided into 10 groups with 12 images in each group. Thus a sequence of 10 camera signatures $\{K_{C_i}(m), K_{C_i}(2m), \ldots, K_{C_i}(rm)\}$ were obtained for each camera device, where r=10 and m=12.

The choice of 10 groups is to produce a sequence of 10 signatures, $K_{C_i}(jm)$ for each camera (j is from 1 to 10). In this way, information with these 10 signatures can be used for source camera identification. In traditional source camera identification, only one camera signature is needed in which the camera signature is obtained from 30 flat images. For seam-carved photos, as demonstrated in Figs 4(c) and 4(d) in Section 3, reliable identification cannot be achieved with only 30 flat images. Here we assume we have 120 images for each camera device. Despite that, as shown in Fig 4(c), the PCE values are still below 50 when 120 images are used for constructing one camera signature for source identification in seam-carved photos. Thus, these 120 images are used to construct 10 fingerprints to study the trend of the PCE values. If more images are available, more camera signatures can be constructed to improve reliability. However, this might affect the practicality of the algorithm as a large number of images are needed to produce the sequence of camera signatures.

Table 1. List of camera devices from different brands and models used in the experiments. Details such as image resolution and format, the number of flat images (#Flat), and the number of natural images (#Nat) are also given.

Labeled	Camera Model	Image Resolution	#Flat	#Nat	File Format
C_1	LG_D290	3264x2448	70	50	JPEG
C_2	Apple_iPhone5c	3264x2448	70	50	JPEG
C_3	Canon_Ixus_55_0	3264x2448	70	50	JPEG
C_4	Sony_XperiaZ1	5248x3936	50	70	JPEG
C_5	Apple_iPad2	960x720	50	70	JPEG
C_6	Fujifilm_FinePix_J50_0	3264x2448	50	70	JPEG
C_7	Asus_Zenfone2Laser	3264x1836	50	70	JPEG
C_8	Nikon_Coolpix_S710_0	4352x3264	50	70	JPEG
C_9	OnePlus_A3000	4640x3480	70	50	JPEG
C_{10}	Huawei_Honor5c	4160x3120	50	70	JPEG
C_{11}	Samsung_GalaxyS4Mini	3264x1836	50	70	JPEG
C_{12}	Samsung_NV15_0	3648x2763	50	70	JPEG
C_{13}	Samsung_NV15_1	3648x2763	50	70	JPEG

5.2 Overall Performance of Cam_{1D}

Each test image was seam-carved to produce two images for evaluation. The first seam-carved image was produced by ensuring that there is at least one seam in every 50 × 50 image block. The second seam-carved image was produced using the forced seam carving method, i.e., there is at least one seam in every 20 × 20 image block. The choice of 20 × 20 blocks, rather than 25 × 25, was to make the evaluation more challenging. While the 20 × 20 image block can help anonymize the source camera information in the test photo, it may also affect the image quality by introducing artifacts. Fig 9 shows an example. We can see that seam carving may introduce visual distortions. For example in Fig 9(d), the wheels are distorted as indicated by the "arrows" in the diagram.

(a) (b) (c) (d)

Fig 9: Forced seam carving in which there is at least one seam in every 20 × 20 image block. The original images are in (a) and (c) while the seam-carved images are in (b) and (d). For the first pair of images in (a) and (b), the image structure is not affected after seam-carving. However, for the image in (d), visual distortion can be seen after seam-carving.

Table 2 shows the confusion matrix for the average results obtained. The columns represent the predicted classes while the rows represent the actual classes. Note that our test images contain different backgrounds with varying content complexity. The accuracy ranged from 87% to 99% with a mean of 95%.

PCE values are often used for source camera identification. A PCE value larger than 50 can be used as a criterion to determine if the test photos come from the same camera as the camera signature (i.e., the matched case). In constructing a reliable camera signature PRNU, the number of photos has to be at least 30. As a comparison with our results in Table 2, the PCE values are obtained to see if reliable source camera identification can be achieved for those seam-carved photos. Fig 10 shows the maximum PCE values for N=60, 72, 84, 96, 108, and 120 for each camera in the matched case.

From Fig 10, we can see that the largest PCE values for all cameras are always smaller than 50. Hence, it is difficult to have a reliable source camera identification on these seam-carved photos using a single PCE value, even though the camera signature was constructed using 120 photos. In contrast, our proposed feature-based method uses a set of camera signatures. The average accuracy on the same set of seam-carved photos is 95%.

In addition to accuracy, the precision, recall, and F1 scores are also important measures. Fig 11 shows these measures for different cameras of our proposed method Cam_{1D}. For most of the cameras, the F1 score, recall, and precision are above 0.9. C_1 and C_8 have a slightly lower value of around 0.88. This is mainly due to the effect of the scene content. The extracted blocks for testing in these two cameras have lower average intensity values and complicated textures like that in Fig 9(e). Currently, we only consider variance in selecting the block while ignoring the image intensity. More study is required to investigate how the block should be extracted. As shown in (Liu et al 2021), patch selection is important for camera identification. In the future, we plan to investigate the extraction of multiple blocks to improve reliability. However, the use of multiple blocks could increase the computational complexity which requires further investigation.

Table 2. Confusion matrix for source camera identification of seam-carved images

Actual \ Predicted	C_1	C_2	C_3	C_4	C_5	C_6	C_7	C_8	C_9	C_{10}	C_{11}	C_{12}	C_{13}
C_1	**87.97**	0.00	0.00	5.19	0.00	0.00	0.53	0.00	0.00	0.00	1.41	4.90	0.00
C_2	1.24	**90.13**	0.00	0.00	6.22	0.26	0.00	2.15	0.00	0.00	0.00	0.00	0.00
C_3	0.16	0.00	**95.45**	0.00	0.00	0.00	0.38	0.00	0.13	1.72	2.16	0.00	0.00
C_4	0.32	0.00	0.00	**94.59**	0.00	0.48	0.00	0.00	0.38	3.18	0.00	0.00	1.05
C_5	0.00	4.89	0.00	0.00	**91.66**	0.00	0.00	0.88	2.48	0.09	0.00	0.00	0.00
C_6	0.01	0.93	1.21	0.00	0.00	**96.96**	0.00	0.21	0.00	0.00	0.00	0.00	0.68
C_7	0.00	0.00	0.00	0.66	0.00	0.00	**99.08**	0.09	0.05	0.00	0.00	0.12	0.00
C_8	0.22	0.90	0.00	0.00	0.67	0.12	0.00	**89.79**	0.00	1.96	2.33	0.00	4.01
C_9	0.00	0.00	1.01	0.00	0.00	0.00	.09	0.36	**98.52**	0.02	0.00	0.00	0.00
C_{10}	1.82	0.00	0.00	0.00	0.00	0.00	0.55	1.31	0.00	**96.32**	0.00	0.00	0.00
C_{11}	0.00	0.00	0.14	0.10	0.00	0.00	0.00	0.00	0.00	0.00	**98.80**	0.61	0.35
C_{12}	0.00	0.00	0.00	0.00	0.00	0.00	0.07	0.02	0.00	0.00	0.29	**99.38**	0.24

C_{13}	0.00	0.00	0.00	0.00	0.00	0.00	0.11	0.09	0.00	0.00	0.44	0.58	**98.78**

Average (%) | **95.19**

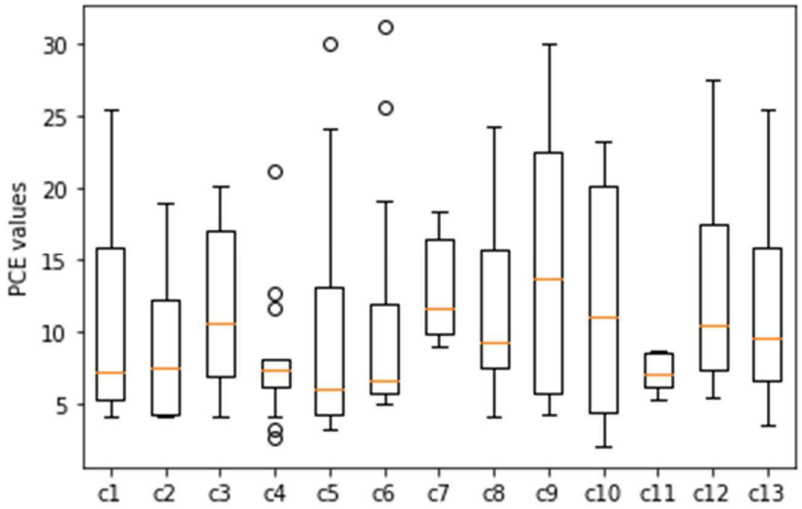

Fig 10: The maximum PCE values of seam-carved photos when *N*=60, 72, 84, 96, 108, and 120 for each camera in the matched case.

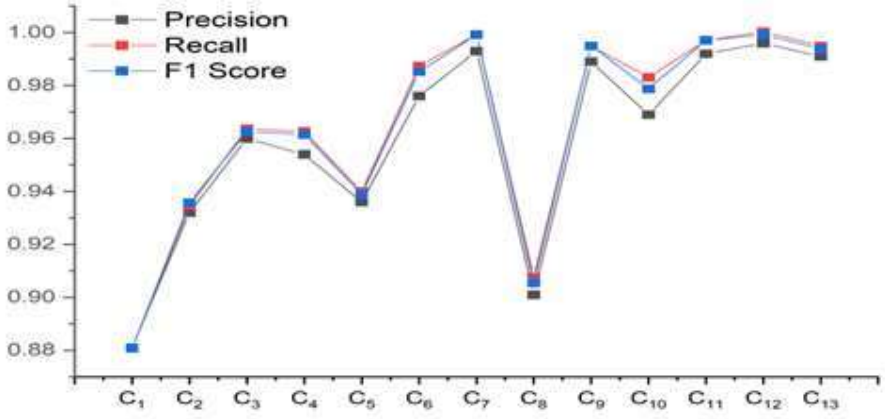

Fig 11: Precision, recall, and F1 scores for the 13 cameras.

5.3 Ablation analysis on the size of the block P

As stated in Section 4.2, a block *P* of size 128 x128 is selected for feature extraction. Ideally, this block should contain uncarved sub-blocks so that the positional correspondence with the camera signature can be established. Seams are located in low-energy regions and are scene-content dependent. For the two types of seam-carving (i.e., 1: one seam in every 50×50 image block and 2: one seam in every 20×20 image block), we study the change in the PCE values when the size of block *P* changes. Fig 12 shows the plots of the PCE values for three different block sizes: 128×128, 50×50, and 25×25 for the two seam-carving cases.

The PCE values for the first type (one seam in every 50×50 image block) are larger than the second type (one seam in every 20×20 image block). It is because the uncarved block size is larger which gives a better positional correspondence with the camera signature. However, for both types, we observed that the PCE values drop when the size of the block decreases for all three cameras. Hence it is more advantageous to use the size 128×128 than the smaller sizes. We could increase the block size at the expense of computational complexity. However, as the performance of 128x128 is good, we fix the block size to 128×128.

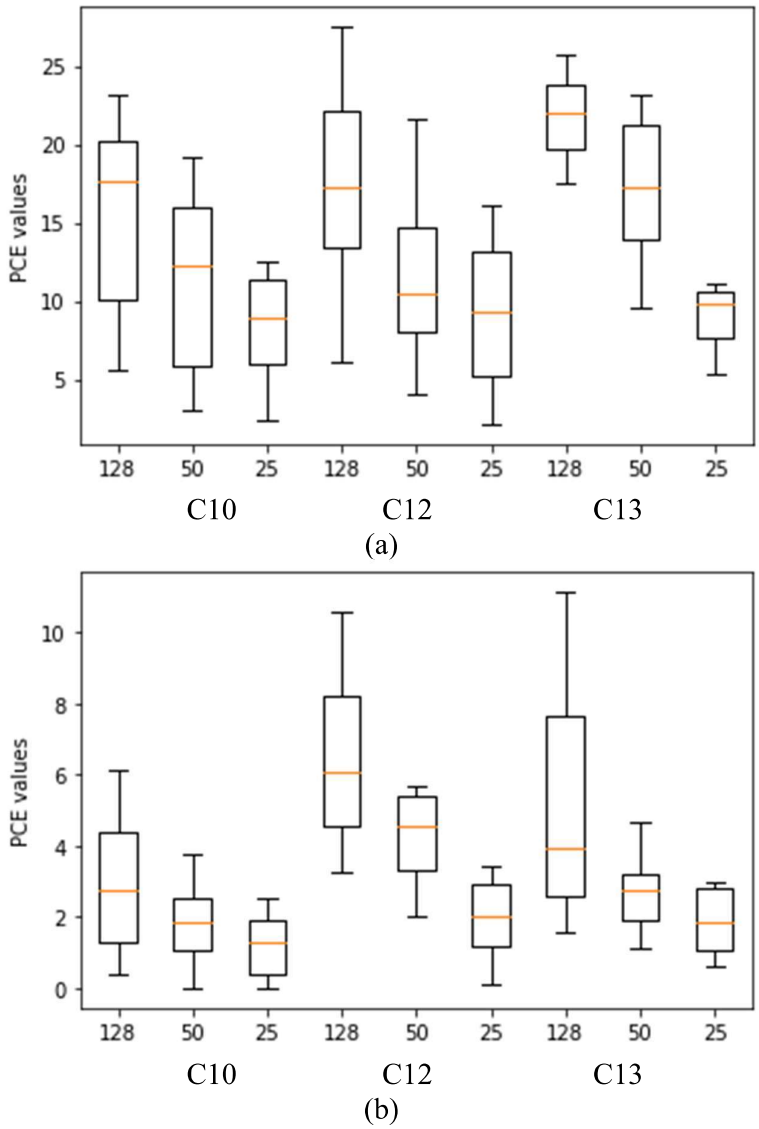

Fig 12: Distribution of the PCE values for the block sizes 128×128, 50×50, and 25×25 for the two types of seam-carving, (a) one seam in every 50×50 image block and (b) one seam in every 20×20 image block.

6. Conclusions

Source camera identification in digital photos that have been resized by seam-carving is an important but challenging task. In prior research, identification was accomplished by detecting either 1) a 50×50 uncarved block in a seam-carved photo or 2) multiple uncarved blocks, smaller than 50×50, from one or more seam-carved photos. The current study aims to determine if reliable source camera identification is possible using a single image with an uncarved block smaller than 50×50.

Our proposed method contains two key components: 1) block selection and 2) feature extraction. Seams are often located in low-energy regions. As such, uncarved blocks can only be found in high-energy regions. Gradient magnitude is thus used to identify potential uncarved blocks. Based on our preliminary studies, we propose that a sequence of camera signatures can offer more reliable information than one camera signature. By analyzing this sequence of camera signatures, we observed an upward trend in correlation values when the seam-carved photo was taken using the same camera. Conversely, random values were obtained when the photo was captured using a different camera. We then extracted five features from the sequence of camera signatures, which allowed us to establish a connection between the seam-carved image and its source camera.

Our proposed method CAM_{ID} was validated using a dataset containing both smartphones and digital cameras. Prior research found that source anonymization is effective, especially if there is at least a seam located in every 25 × 25 image block. Our experimental results demonstrate that a single PCE value cannot be used to reliably identify the source camera in a seam-carved photo. However, the proposed method can achieve more reliable results. We plan to create a dataset of seam-carved images with source camera information, which will facilitate large-scale testing in the future.

ACKNOWLEDGEMENTS

This work was supported by the GRF Grant 15211720 (project code: Q79N) of the Hong Kong SAR Government. Muhammad Irshad Ibrahim would like to thank the postdoctoral fellowship support from Hong Kong Polytechnic University (GYW4X). The authors would like to thank the reviewers for their constructive comments that have greatly improved the paper.

Availability of data and material: All datasets used are public datasets.

REFERENCES

Younes Akbari, Somaya Al-maadeed, Omar Elharrouss, Fouad Khelifi, Ashref Lawgaly, Ahmed Bouridane, “Digital Forensic Analysis for Source Video Identification: A Survey”, *Forensic Science International: Digital Investigation* 41, (2022), 301390.

S. Avidan and A. Shamir, “Seam Carving for Content-Aware Image Resizing.” *Proceedings of the ACM SIGGRAPH Conference on Computer Graphics* 26(3), (2007).

S. Bayram, T. Sencar, and N. D. Memon, “Seam-Carving Based Anonymization against Image & Video Source Attribution”, *2013 IEEE International Workshop on Multimedia Signal Processing,* (2013), 272–277.

Jaroslaw Bernacki, “A Survey on Digital Camera Identification Methods”, *Forensic Science International: Digital Investigation* 34, (2020) 300983.

Gajanan K. Birajdar and Vijay H. Mankar, “Digital Image Forgery Detection Using Passive Techniques: A Survey”, *Digital Investigation* 10(3), (2013) 226–245

L.H. Chan, N.F. Law and W.C. Siu, "A Confidence Map and Pixel-Based Weighted Correlation for PRNU-Based Camera Identification", *Digital Investigation* 10(3), (2013), 215–25.

M. Chen, J. Fridrich, M. Goljan, and J. Lukáš, "Determining Image Origin and Integrity Using Sensor Noise", *IEEE Transactions on Information Forensics and Security* 3(1), (2008), 74–90.

A.E. Dirik, H.T. Sencar and N. Memon, "Analysis of Seam-carving-based Anonymization of Images against PRNU Noise Pattern-based Source Attribution, *IEEE Transactions on Information Forensics and Security*, 9(12), (2014), 2277-2290.

M. Frankovich and A. Wong, "Enhanced Seam Carving via Integration of Energy Gradient Functionals." *IEEE Signal Processing Letters* 18(6) (2011), 375–378.

T. Gloe and R. Böhme, "The 'Dresden Image Database' for Benchmarking Digital Image Forensics." *Proceedings of the 2010 ACM Symposium on Applied Computing - SAC '10*, (2010)

M. Goljan, J. Fridrich and T. Filler, "Large scale test of sensor fingerprint camera identification", Media Forensics and Security, (2009), 725401 – 72540I-12.

M. Irshad, N.F. Law, and K. H. Loo, "CamCarv - Expose the Source Camera at the Rear of Seam Insertion." , L. Rutkowski Et al. (Eds): ICAISC 2022, LNAI 13589, (2023), 21-34.

X. Kang, Y. Li, Z. Qu, and J. Huang, "Enhancing Source Camera Identification Perofmrnace with a Camera Rference Phase Sensor Pattern Noise", *IEEE Transactions on Information Forensics and Security*, Vol. 7, (2012), 393-402.

K.F. Lau, N.F. Law and W.C. Siu, "Use of Sensor Noise for Source Identification", *International Conference on Noise Fluctuations*, June 2015.

Sai Chung Law and N.F. Law, "Performance enhancement of PRNU-based Source Identification for Smart Video Surveillance", *HKIE Transactions*, Vol. 29, Issue 3, (2022), 172-181.

Liu, Yun Xia, Ngai Fong Law, and Wan Chi Siu, "Patch Based Image Denoising Using the Finite Ridgelet Transform for Less Artifacts", *Journal of Visual Communication and Image Representation* 25(5), (2014), 1006–17.

Yun-Xia Liu, Zeyu Zou, Yang Yang, N.F. Law and Anil Anthony Bharath, "Effective Source Camera Identification with Diversity Enhanced Patch Selection and Deep Residual Prediction", Sensors 21 (14): 4701, 2021

J. Lukáš, J. Fridrich, and M. Goljan, "Digital Camera Identification from Sensor Pattern Noise", *IEEE Transactions on Information Forensics and Security* 1(2), (2006), 205–14.

D. Minnen, G. Toderici, S. Singh, S. J. Hwang, M. Covell "Image-Dependent Local Entropy Models for Learned Image Compression." *Proceedings – International Conference on Image Processing, ICIP*, (2018) 430–34.

C. Shi, N.F. Law, F.H.F. Leung, and W. C. Siu, "A Local Variance Based Approach to Alleviate the Scene Content Interference for Source Camera Identification", *Digital Investigation* 22, (2017) 74–87.

D. Shullani, M. Fontani, M. Iuliani, O. AI Shaya and A. Piva, "VISION: A Video and Image Dataset for Source Identification." *EURASIP Journal on Information Security 2017:1* 2017(1), (2017), Article Number: 15.

S. Taspinar, M. Manoranjan and N. Memon, “PRNU Based Source Attribution with a Collection of Seam-Carved Images”, *Proceedings - International Conference on Image Processing, ICIP* (2016), 156–160.

S. Taspinar, M. Manoranjan and N. Memon, “PRNU-Based Camera Attribution from Multiple Seam-Carved Images”, *IEEE Transactions on Information Forensics and Security* 12(12), (2017), 3065–3080.